Supplement to the Annual Report for FY06

Supplemental information to the Annual Report November 2006

Environmental Molecular Sciences Institute support for the Center for Environmental Molecular Sciences

C. Dodge, J. Fitts, A.J. Francis, M. Fuhrmann, J. Gillow, P. Kalb, P. Northrup, D. Chidambaram, G. Crosson
Environmental Sciences Department, Brookhaven National Laboratory Upton, NY 11973

Chemistry of grout materials used to stabilize radionuclides

Mark Fuhrmann[1,3]*, P. Northrup*[1,3] *and J. Parise*[2,3]
[1]Environmental Sciences Department, Brookhaven National Laboratory
[2]Department of Geosciences, Stony Brook University
[3]Center for Environmental Molecular Sciences, Stony Brook University

This project is investigating the chemical processes that govern actinide sequestration in grout materials with the goal of determining the long-term behavior of grouts used to stabilize actinides in source-terms such as high level waste tank heals. Two grouts contained portland cement, blast furnace slag and fly ash, with one formulation containing zeolite and the other fluorapatite. Earlier experimental work was conducted with funds from DOE/West Valley. CEMS funding allowed further exploration of grout behavior, beyond the scope of the original work which consisted of both batch and flow-through column experiments. The primary focus was the late stage behavior of actinides in the grout system when it is expected to be open to the atmosphere and groundwater, resulting in decreases of pH and interactions of U (and other elements) with dissolved carbonate.

Initially the solubility of contaminants will be constrained by chemistry dominated by the grout, primarily by the high pH, around 12. This is controlled and buffered by the portland cement and blast furnace slag components of the grout, which by themselves maintain a solution pH of about 12.5. Slowly the pH will diminish as $Ca(OH)_2$ and KOH dissolve, are carried away by water, and $CaCO_3$ forms. As these conditions develop, the behavior of U comes into question.

The behavior of uranium in contact with two grouts formulated as potential backfill materials for emptied high-level radioactive waste facilities was investigated through a set of batch experiments, some extending up to 550 days. Solution U(VI) concentrations generally remained below the detection limit of 0.3 mg/L when access to atmospheric CO_2 was limited. As $KHCO_3$ was added to simulate weathering effects, U(VI) was released to solution but concentrations were limited to 3 mg/L or less for grouts and grout materials that maintained pH greater than 11.5. At pH values lower than 11.5, higher U(VI) concentrations were sometimes observed. Calcite was an important secondary mineral even when CO_2 was limited, and uranium partitioned into the calcite, resulting in concentrations as high as 9,600 mg/kg. Evidence from these batch experiments, supported by solid phase analysis, shows that partitioning of uranium to calcite is an important control on the long-term fate of U(VI), in a near-surface grout system. Uranium and the other elements that partition into calcite (e.g., As) may be effectively sequestered even in the end-state of the disposal system when it is open to dissolved carbonate. This takes place in static conditions, but does it also occur in dynamic systems?

A set of column experiments allowed an assessment of changing U concentrations, pH and other chemical parameters, over time, as simulated West Valley groundwater flowed through the grouts. Over the coarse of 1000 pore volumes of leaching, less than 10% of the U was released from the grouts. In fact over time effluent concentrations of U peaked at between 40 and 70 ppb and then began to decrease. Synchrotron microprobe (NSLS beamlines X-26 and X27A) showed that U was incorporated into authigenic calcite forming in the columns, much as it did under static conditions. Some of the U was mobilized into the solution but most of it was reincorporated into the grout. Geochemical modeling, constrained by elemental concentrations and pH measured in the column effluent, indicates that there is enough Si in solution that around pH 9 the uranium silicate soddyite is super saturated. This conforms to the observation of decreased U in the column effluent. SEM work indicates that P was mobilized during leaching and solids containing Ca, Si and P were common in the leached grout column. It may be that U has reacted with P to form very low solubility phosphate minerals. Microprobe observations show that U was incorporated into calcite for only a portion of the time that the calcite was forming even though As was incorporated throughout the deposition of the calcite. This is shown in figure 1. The chemistry of U remobilization and sequestration into secondary phases is critically important in understanding the long-term behavior of these materials. This process is the focus of the current work in this project.

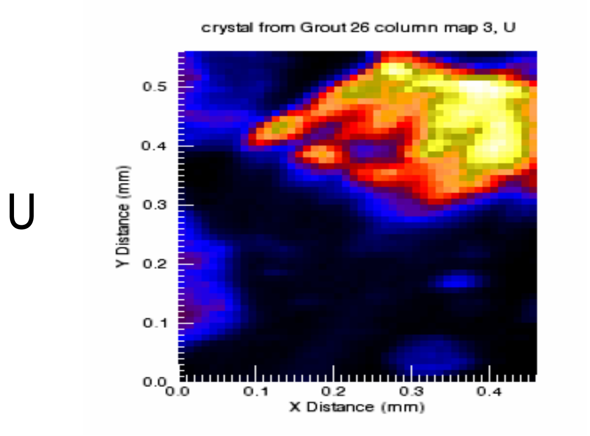

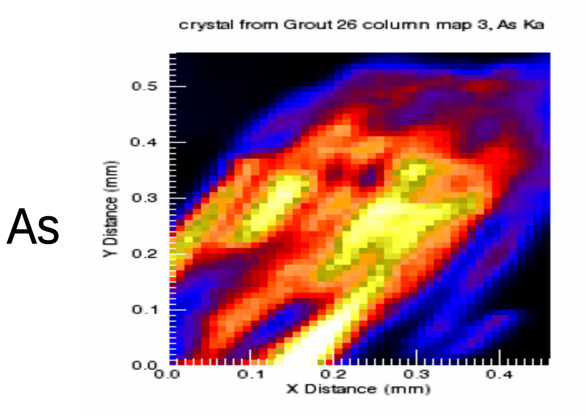

Figure 1. The distributions of As and U are shown in a calcite crystal from a flow-through experiment. A photo of the particle is shown above. While arsenics is distributed throughout the particle uranium is only present in its top portion, indicating that it was not

Structural Characterization of Actinides Associated with Organic Ligands

Cleveland J. Dodge[1,3], G. Halada[3], B. Philips[2,3] and Arokiasamy J. Francis[1,3]
[1]Environmental Sciences Department, Brookhaven National Laboratory
[2]Department of Geosciences, Stony Brook University
[3]Center for Environmental Molecular Sciences, Stony Brook University

RESEARCH OBJECTIVES:

The objectives of this research are to (i) establish the molecular structure of actinides (e.g. U, Pu) with naturally-occurring complexing agents catechol, oxalate and citrate; (ii) determine the actinide association with synthetic organic ligands present in Hanford tank wastes, contaminated soils obtained from the Rocky Flats Environmental Technology Site (RFETS), Rocky Flats, CO, and the Nevada Test Site (NTS); (iii) investigate the influence of multiple ligands on actinide complexation; and (iv) determine the selectivity and stability of the resulting complexes.

RESEARCH PROGRESS AND IMPLICATIONS:

Molecular structure determination of U:catechol complex. Catechol, a structural component of natural organic matter (NOM), forms soluble complexes with uranyl ion. We determined the nature of the complex species formed as a function of pH 3.0, 4.0, 5.0, and 6.0 using a combination of analytical techniques including electrospray ionization-mass spectrometry (ESI-MS) and X-ray absorption spectroscopic (XAS) analysis. The association of uranium with the ligand was influenced by the pH of the solution (Figure 1). At pH 3.0 the monomeric form [UO_2cat] was predominant (Figure 1A). With an increase in pH to 4.0 and 5.0 a dimeric complex [$(UO_2)_2(\mu_2\text{-}OH)cat_2$] (Figure 1B) and a triligand complex [$(UO_2)_2(OH)$cat$_3$] were observed. At pH 6.0 a trimeric [$(UO_2)_3$cat$_3$] complex was formed due to polymerization of the U-catechol. In this structure two catechols are bound in bidentate fashion to the trimeric uranium core, while the third catechol forms a monodentate complex with the second uranyl ion. UV-vis spectrophotometry and particle size analyses confirmed that polymerization of the complex occurs at the higher pH's ($\geq$ 6). These results present the first systematic structural study of the effect of pH on U-catechol complex formation and suggest that catechol can affect the speciation and mobility of uranium in the environment.

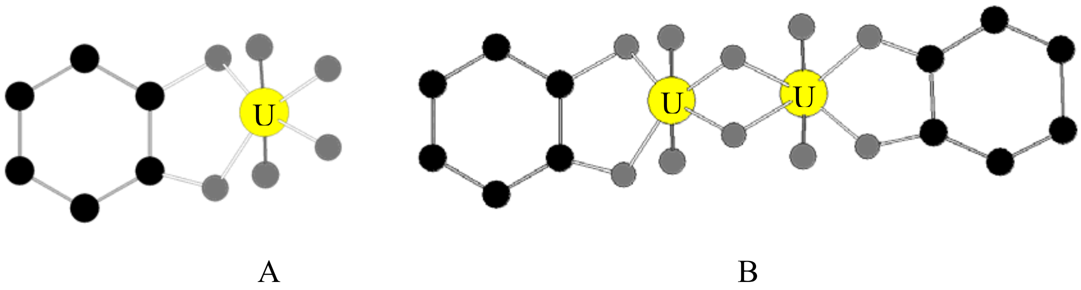

Figure 1. Proposed structures for the monomeric (A) and the dimeric (B) complexes of uranium with catechol. Atoms: gray, O; black, C.

Structural characterization of actinide-mixed ligand complexes. The presence of actinides and multiple ligands in solution may lead to the formation of mixed-ligand complexes. Mixed-ligand complexes are of particular interest because of their unique chemical properties compared to monoligand forms. Increased stability as well as mobility of mixed-ligand complex systems may result in mobilization of the actinide away from the waste site. In the following studies we determined the molecular association and stability of Eu^{3+} (an analog for Pu^{3+}) with ligands nitrilotriacetic acid (NTA), ethylenediamine tetraacetic acid (EDTA), and oxalic acid (Ox).

Eu:EDTA:NTA complexes. The formation and molecular structure of the ternary complexes of trivalent Eu, Am, and Cm with mixtures of EDTA+NTA have been studied by TRLFS, ^{13}C NMR, EXAFS and the two phase metal ion equilibrium distribution at I= 6.60 mol/kg^{-1} ($NaClO_4$) and pcH between 3.6 to 11.5. In the ternary complexes, EDTA binds via four carboxylate oxygens and two nitrogens, and NTA via 2 or 3 sites, depending on the concentration ratio of metal ions and EDTA and the pcH of the solution. For ratios of M:EDTA:NTA of 1:1:1 and 1:1:2 and pcH of ~9.0, two ternary complexes are formed with NTA binding via three carboxylates in one and via two carboxylates and one nitrogen or two carboxylates and one H_2O in the other. A single ternary complex $M(EDTA)(NTA)^{4-}$ forms with M:EDTA:NTA of 1:1:20 and 1:10:10 and pcH between 9.0-11.5, and with M:EDTA:NTA of 1:1:1 and 1:1:2 and pcH between 11.1-11.5, in which NTA binds via three carboxylate groups (Figure 2). Two phase equilibrium distribution studies at tracer concentrations of Eu, Am, and Cm also confirmed the formation of the ternary complex $M(EDTA)(NTA)^{4-}$ at temperatures between 0-60 ^{0}C. The stability constants ($\log\beta_{111}$) for these metal ions increase with increasing temperature with values ranging from 25.73 to 25.96 at 25 ^{0}C. The heats of reaction (ΔH_{111}) at high ionic strength, are positive in contrast to the negative values usually observed at lower ionic strengths for these metal ions. This is attributed to the much reduced activity of water at high ionic strengths.

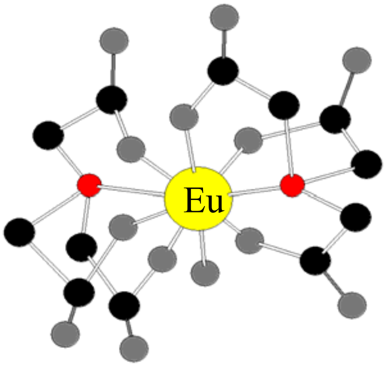

Figure 2. Proposed structure showing the binding modes for the formation of the ternary complex $Eu(EDTA)(NTA)^{4-}$ at Eu:EDTA:NTA of 1:10:10 and pcH 11.5. The EDTA is bound to Eu^{3+} via two nitrogens and four carboxylate groups and NTA via three carboxylate groups. The nitrogen of NTA is not involved in the bonding. Atoms: gray, O; black, C; red, N.

Eu:EDTA:Ox complexes. In the presence of EDTA and oxalate EXAFS data analysis confirmed Eu forms a $Eu(EDTA)(H_2O)^{3-}$ complex in which EDTA binds *via* four carboxylate groups and two nitrogens which is consistent with XRD analysis. The best fit of the EXAFS data for the 1:1:1 Eu-EDTA-Ox complex indicates 7.0 ± 1.2 oxygens at 2.43 ± 0.01 Å, 6.3 ± 1.5 carbons at 3.24 ± 0.04 Å and 1.8 ± 0.04 nitrogen atoms at 2.80 ± 0.05 Å. These data lead to a total coordination number (CN) of 8.8 (1EDTA (4 carboxylates + 2 nitrogens) + 1 Ox] (2 carboxylates) + $1H_2O$) for Eu^{3+} in $Eu(EDTA)(Ox)(H_2O)^{3-}$. The TRLFS data of *ca.* 1.5 ± 0.5 waters of hydration in the complex $Eu(EDTA)(Ox)^{3-}$ is substantiated by the EXAFS data. At Eu:EDTA:Ox of 1:1:2, the EXAFS analysis establishes the formation of a ternary complex $Eu(EDTA)(Ox)_2^{5-}$. The EXAFS best fit data of 7.2 ± 1.4 oxygens at 2.43 ± 0.02 Å , 7.5 ± 1.5 carboxylate carbons at 3.22 ± 0.03 v and 2.0 ± 0.5 N atoms at 2.78 ± 0.04 Å suggest a total CN = 9.2 for Eu^{3+} in $Eu(EDTA)(Ox)_2^{5-}$. The presence of 7.5 ± 1.5 carboxylate carbons indicates that one of the carboxylate groups of either EDTA or oxalate remains unbound in the ternary complex, $Eu(EDTA)(Ox)_2^{5-}$. Although the EXAFS data are consistent with the results of TRLFS and NMR (^1H and ^{13}C), the TRLFS results of *ca.* 0.9 ± 0.5 waters of hydration in the ternary complex $Eu(EDTA)(Ox)_2^{5-}$ are contrary to those of the EXAFS studies. Since both EDTA and oxalate are hard base donors and show greater preferences for the hard acid cation like Eu^{3+}, it is reasonable to assume that the ternary complex $Eu(EDTA)(Ox)_2^{5-}$ has no water of hydration attached to the inner coordination sphere of Eu^{3+}. It may be likely that the usually hexadentate EDTA behaves as a pentadentate ligand, allowing higher coordination for the oxalate ligands in the ternary complex. Fig. 3A shows the association of Eu^{3+} with EDTA and oxalate in the formation of ternary 1:1:1 complex, $Eu(EDTA)(Ox)(H_2O)^{3-}$. We cannot unambiguously assign the structure of the ternary 1:1:2 complex (Figure 3B). The stability constants and the associated thermodynamic complex based on this study, however, it has been proposed that the coordination modes of the ternary 1:1:2 complex are similar to that of the 1:1:1 complex; with one of the carboxylates from EDTA or oxalate remaining unbound and no water of hydration associated with the Eu^{3+}. Further research on the crystal structure of the solid compounds and/or solution is required to determine the exact structure.

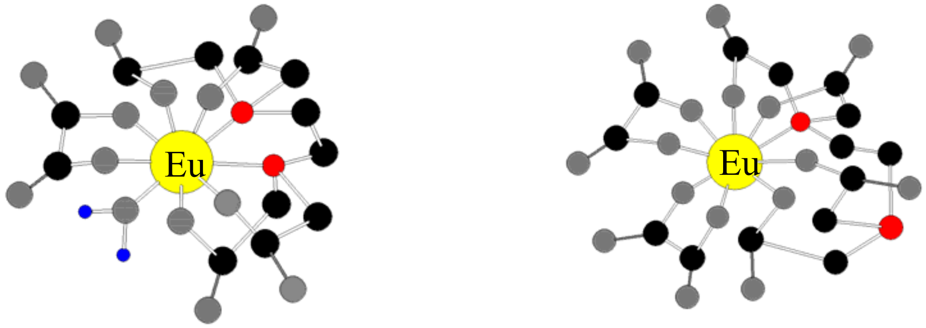

Fig. 3. Proposed molecular structures for 1:1:1 Eu:EDTA:Ox (A) and 1:1:2 Eu:EDTA:Ox. Atoms: gray, O; black, C; blue, H; red, N.

Spectromicroscopy of Environmental Microbial Processes

J.B. Gillow[1,3], B. Larson[2,3], J. Fitts[1,3], S. Wirick[2,3] , A.J. Francis[1,3], and C. Jacobsen[2,3]
[1]Environmental Sciences Department, Brookhaven National Laboratory
[2]Department of Physics and Astronomy, Stony Brook University
[3]Center for Environmental Molecular Sciences, Stony Brook University

The objective of this project is to use scanning transmission x-ray spectromicroscopy (STXM) at beamline X1A at the NSLS to obtain molecular chemical information about subcellular features of spore-forming bacteria. Whole *Clostridia* and *Bacillus* cells were prepared at various stages of spore-formation and imaged at the carbon K edge. Cluster analysis, an unsupervised pattern-matching algorithm, was used to identify features in the bacteria based on differences in the carbon chemistry. The interaction of sporulating bacteria, important for many mineral and contaminant transformations in the natural environment, with iron (hydr)oxides was examined using this technique. The anaerobic fermentative bacterium *Clostridium* sp. BC1 was grown in the presence of ferrihydrite to determine what effect the mineral has on the chemistry of the subcellular features, specifically exopolymeric substances (EPS). Samples were prepared at 48 hours and 6 day growth. Figure 1 shows the results of using cluster analysis on the 48-hour sample, with a carbon K-edge false-color map inset on the absorption spectra correlated to the colors in the map. The analysis picked out shifts in the C=O peak around 288 eV. The yellow cluster is the bacterium, the red is most likely the exopolymer, and the green and purple clusters correspond to areas where the ferrihydrite is interacting with the exopolymer at the iron oxide-organic carbon interface. Figure 2 shows an electron micrograph of the *Clostridum* sp. grown in the presence of ferrihydrite at pH 3.

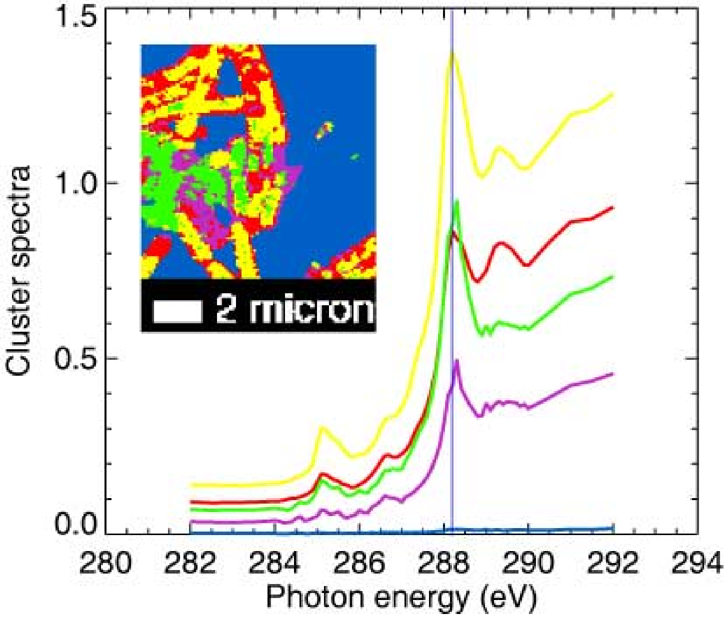

Figure 1. Carbon K-edge scanning transmission spectromicroscopy (STXM) of the interaction of *Clostridium* sp. with ferrihydrite. Inset shows a false-color map of the bacterial cells and EPS-coated iron oxide with corresponding K-edge absorption spectra.

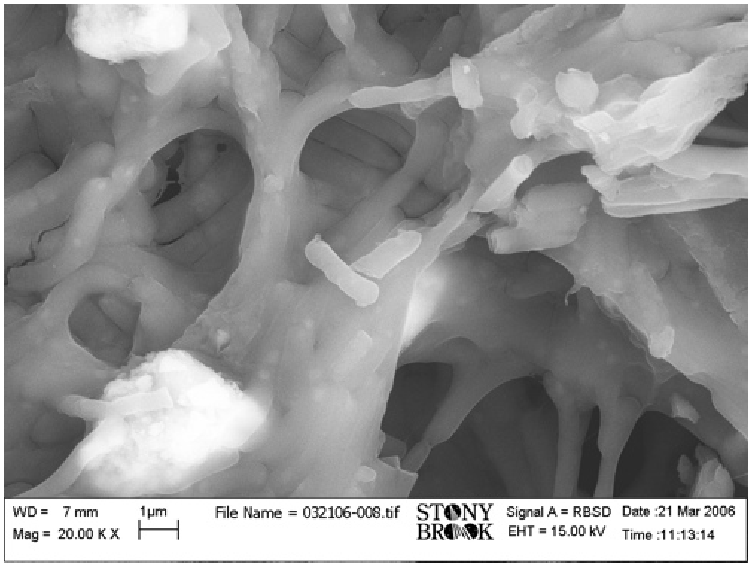

Figure 2. Scanning electron micrograph of Clostridium sp. bacterial cells grown in the presence of ferrihydrite for 48 hours. The whole bacterial cells are clearly visible embedded in EPS surrounding the ferrihydrite particles (large bright particles).

The scanning electron microscopy analysis supports the results of the STXM study, providing evidence of the EPS coating the ferrihydrite particles. The STXM interaction provides information relative to the chemical interaction of the EPS with the ferrihydrite particles. This is found to play a role in preventing the dissolution of the ferrihydrite at low pH due to passivation by the EPS and specifically organic carbon and phosphate sorption, due to phosphate groups present in the EPS. The iron L edge on the inboard branch of X1A was used to examine the differences in iron chemistry between the two samples and compare these with standard iron oxides. Ferrihydrite is a naturally-occurring nanoparticulate iron (hydr)oxide and can be used as a natural analog for the study of biofilm-nanoparticle interactions to understand how microbial processes affect the fate and transport of engineering (anthropogenic) nanoparticles. This is currently being studied using STXM; the interaction of engineered nanoparticles and soil bacteria to determine the fate of nanoparticles in the environment. In preliminary studies, *Pseudomonas fluorescens* was grown in the presence of gold nanoparticles. These samples were imaged at the carbon edge. The goals for this work during the next year include 1) understanding the chemical basis for the unique carbon K-edge spectra of EPS-ferrihydrite interactions, 2) analysis of the iron oxide at the iron L edge to identify biotransformed mineral phases, and 3) obtaining a molecular-chemical understanding of microbial interactions with engineered nanoparticles, developed in tasks (1) and (2), in order to identify the mechanism of interaction between soil biofilms and nanomaterials in the environment.